Separation Science and Technology
Publication details, including instructions for authors and subscription information:
http://www.informaworld.com/smpp/title~content=t713708471

Adsorption Characteristics of Toluene and *p*-Xylene in a Reversed-Phase C_{18} Column for Simulated Moving Bed Chromatography

Youn-Sang Bae[a]; Sung-Ha Im[a]; Kang-Man Lee[a]; Joong Kee Lee[b]; Chang-Ha Lee[a]
[a] Department of Chemical Engineering, Yonsei University, Seoul, Korea [b] Eco-Nano Technology Research Center, Korea Institute of Science and Technology, Seoul, Korea

To cite this Article Bae, Youn-Sang , Im, Sung-Ha , Lee, Kang-Man , Lee, Joong Kee and Lee, Chang-Ha(2005) 'Adsorption Characteristics of Toluene and *p*-Xylene in a Reversed-Phase C_{18} Column for Simulated Moving Bed Chromatography', Separation Science and Technology, 40: 11, 2183 — 2204
To link to this Article: DOI: 10.1080/01496390500201151
URL: http://dx.doi.org/10.1080/01496390500201151

Separation Science and Technology, 40: 2183–2204, 2005
Copyright © Taylor & Francis, Inc.
ISSN 0149-6395 print/1520-5754 online
DOI: 10.1080/01496390500201151

Adsorption Characteristics of Toluene and *p*-Xylene in a Reversed-Phase C_{18} Column for Simulated Moving Bed Chromatography

Youn-Sang Bae, Sung-Ha Im, and Kang-Man Lee
Department of Chemical Engineering, Yonsei University, Shinchon-dong, Seodaemun-gu, Seoul, Korea

Joong Kee Lee
Eco-Nano Technology Research Center, Korea Institute of Science and Technology, Hawolgok-dong, Sungbuk-gu, Seoul, Korea

Chang-Ha Lee
Department of Chemical Engineering, Yonsei University, Shinchon-dong, Seodaemun-gu, Seoul, Korea

Abstract: The adsorption equilibria and transport properties of toluene and *p*-xylene on a Eurosil 100-30-C_{18} column were measured from a chromatographic response in a reversed-phase HPLC. Moment method was applied to the effluent peaks obtained from various temperatures and eluent compositions. The adsorption equilibrium constants were obtained from the first moment analysis. On the other hand, the transport properties such as the axial dispersion coefficient and effective diffusivity were obtained from the second moment analysis. The simulated results of the simulated moving bed process using the parameters obtained from the moment analysis agreed well with the experimental results. And the separation of toluene/*p*-xylene mixture could be successfully separated by the simulated moving bed process.

Keywords: Chromatography, C_{18} column, column liquid chromatography, moment method, simulated moving bed

Received December 9, 2004, Accepted May 24, 2005

Address correspondence to Chang-Ha Lee, Department of Chemical Engineering, Yonsei University, Shinchon-dong, Seodaemun-gu, Seoul 120-749, Korea. Tel.: +82-2-2123-2762; Fax: +82-2-312-6401; E-mail: leech@yonsei.ac.kr

INTRODUCTION

High-performance liquid chromatography (HPLC) is one of the most powerful and reliable separation methods in most fields of chemistry and chemical engineering. In the field of analytical liquid chromatography, the reversed-phase technique is most frequently employed. It is estimated that 70 to 80% of chromatographic separations on analytical works have been carried out in a reversed-phase mode (1–3).

Equilibrium isotherms and transport properties are the most important characteristics for understanding and designing chromatographic processes such as preparative HPLC and simulated moving bed (SMB) (4–6). Numerous methods have been developed for the experimental determination of equilibrium isotherm and transport parameters (7). The moment method is one of the most basic strategies for determining the equilibrium and transport parameters when the system isotherm is linear (1).

For the optimal separation of mixture on a reversed-phase HPLC column, the composition of mobile phase, flow rate, column packing density, and particle porosity need to achieve the proper resolution and complete separation of desired solutes.

In this study, the equilibrium and kinetic properties between the adsorbent and the adsorbate were obtained from a moment method using HPLC. These properties were applied to accurately determine the adsorption characteristics in the SMB chromatography. Toluene and p-xylene, which are essential constituents of the BTX (benzene, toluene, and xylene) process, were selected as model components to verify the applicability of moment method to the SMB chromatography. The adsorption equilibria and transport properties of toluene and *p*-xylene on a Eurosil 100-30-C_{18} column were measured by using a reversed-phase (RP) HPLC. Since the concentration of adsorbate was small, the moment method could be used. The required information regarding the retention equilibrium and kinetics was derived from the first and second moments. The effects of temperature and mobile phase composition on the adsorption characteristics of toluene and *p*-xylene in the RP-HPLC were also elucidated. Finally, the equilibrium and transport parameters from chromatographic technology were applied to the simulation and experiment for the separation of toluene/*p*-xylene mixture by using a simulated moving bed (SMB) process (8).

EXPERIMENT

Materials

A Eurosil Bioselect column (KNAUER, 25 × 0.8 cm I.D., Germany) packed with silica-based C_{18} was used. To minimize pressure drop in the SMB process, the adsorbent with 30 μm particle size was used (9). Table 1 shows the physical properties of this column.

Table 1. Physical properties of the Eurosil Bioselect 100-30-C_{18} column

Carbon content (%, w/w)	12.5	Particle density, ρ_p (g/cm^3)	0.4
Particle diameter, d_p (μm)	30	Column volume, V_b (cm^3)	12.57
Pore size (Å)	100	Mass of packing materials (g)	8.42
Pore volume, V_p (mL/g)	1.1	Bed density, ρ_b (g/cm^3)	0.67
BET surface area (m^2/g)	385	Bed porosity, ε_b (-)	0.709
Particle porosity, ε_p (-)	0.44	Phase ratio, F (-)	0.410

Toluene (+99.5%) and *p*-xylene (+99%) were purchased from Duksan (Ansan, Korea) and Yakuri (Osaka, Japan), respectively. Table 2 shows the physical properties of toluene and *p*-xylene. Thiourea, nonretained component, was obtained from Duksan (Ansan, Korea).

The mobile phase was a mixture of water (Duksan, HPLC-grade) and methanol (J.T. Baker, HPLC-grade). These solvents were used after further filtration and sonication. A 0.45 μm filter was used to eliminate the particulate matters from each solvent. Table 3 shows the viscosities and densities of pure water and pure methanol at three temperatures. As shown in the table, since the viscosity and density are changed with temperature, these properties were reflected on the calculation of adsorption properties.

Equipment

The chromatographic study was done by a high-performance liquid chromatograph (Waters Breeze, Milford, MA), equipped with a binary HPLC pump (Waters 1525), a UV-visible detector (Waters 2487), a Rheodyne injector with a 20 μL loop, and a column heater. The detector was connected to a computer equipped with a data acquisition system using the Waters® *Breeze™* software. The UV detector was calibrated at 254 nm wavelength for quantification.

A small pilot-scale SMB of the KNAUER CSEP® 9116 (KNAUER, Germany) was used for a continuous separation of toluene/*p*-xylene mixture in this study. The system consisted of eight columns, and the configuration of the eight columns was 2-2-2-2. The Eurosil Bioselect (KNAUER,

Table 2. Physical properties of adsorbates

Properties	Toluene	*p*-Xylene
Molecular weight, M	92.140	106.17
Density, ρ (g/cm^3)	0.870	0.865
Molecular formula	$C_6H_5CH_3$	$C_6H_4(CH_3)_2$

Table 3. Physical properties of pure solvents

Temperature (K)	Properties	Methanol	Water
308.0	Viscosity, μ (cp)	0.462	0.736
	Density, ρ (g/cm^3)	0.778	0.994
315.5	Viscosity, μ (cp)	0.426	0.638
	Density, ρ (g/cm^3)	0.770	0.991
323.0	Viscosity, μ (cp)	0.395	0.559
	Density, ρ (g/cm^3)	0.703	0.988

Germany) columns (25 × 0.8 cm I.D.) packed with silica-based C_{18} packing materials (30 μm) were used. The system was equipped by four HPLC pumps, two flowmeters, and a two-channel degasser. All the columns were kept in the thermostatic column oven (35 × 45 cm). For the analysis of the collected fractions, a Waters symmetry column (15 × 0.45 cm I.D.) packed with silica-based C_{18} packing materials (5 μm) was used.

Procedures

Before each experimental operation, the HPLC system was washed overnight by a mobile phase at a flow rate of 0.1 mL/min for the stability of the system. Then, the system was purged to remove bubbles from the system for a few minutes.

After the pretreatment, the adsorption equilibria and kinetics of toluene and *p*-xylene were investigated by the experiments of chromatographic elution peak. The effects of temperature on adsorption equilibria and kinetics were measured at 308, 315.5, and 323 K. In addition, the measurements were performed at several solvent ratios (70, 80, and 90 vol.% of methanol ratio) to observe the effect of solvent ratio on adsorption properties.

The concentration of each component in the feed mixture was 2 g/L, and 20 μL of the feed mixture was injected to the HPLC system. The equilibria and kinetic parameters were determined from the elution peaks by the moment analysis.

The equilibrium values obtained from the moment method were used to determine the operating condition of the SMB process by the triangle theory. Based on this equilibrium model, explicit expressions of the fluid to solid flow rate ratios, m_j ($j = 1, \ldots, 4$), for the complete separation of binary mixtures were obtained from the true countercurrent (TCC) adsorption model (10–13). The operating condition of the SMB process was then based on the equivalence between the SMB and TCC processes. The explicit criteria were obtained from the boundaries of the complete separation region in the space spanned by m_j ($j = 1, \ldots, 4$). In this study, by this triangle theory, the operating condition (four flow rates and switching time) of the SMB process was determined by the triangle theory (10–13).

Before the SMB operation, the SMB system was washed overnight by a mobile phase at a flow rate of 0.1 mL/min for the stability of the system. Then, the system was purged to remove bubbles from the system for a few minutes. The experiments were done at the following conditions: feed flow rate and concentrations were $Q_F = 1.00\,\text{mL/min}$, $C_{1,F} = C_{2,F} = 2\,\text{g/L}$, respectively. The transient changes of purities and product concentrations of extract and raffinate products were measured by sampling both products at the last switching time of each cycle. Finally, these samples were injected to the HPLC system to obtain their purities and concentrations. For the dynamic simulation of the SMB process, the simulation package gPROMS ModelBuilder 2.3.0. (PSE Ltd., UK) was used.

MATHEMATICAL MODEL

In the chromatographic method, the adsorption characteristics can be determined by measuring the dynamic response of a packed column to the injection of a small pulse of sorbate at the inlet. Such measurements provide the simple and rapid information of adsorption equilibria and kinetics. The mean retention time is directly related to the adsorption equilibrium constant, while the spread of the response peak is related to the combined effects of dispersion and mass transfer resistances (14).

The experimental values of the first absolute and second central moments are obtained from the response curves with the following equations:

$$\mu_1 = \frac{\int_0^\infty t \cdot c(L,t)dt}{\int_0^\infty c(L,t)dt} \tag{1}$$

$$\mu_2' = \frac{\int_0^\infty (t-\mu_1')^2 \cdot c(L,t)dt}{\int_0^\infty c(L,t)dt} \tag{2}$$

Using these equations, Kubin (1965) (15) and Kučera (1965) (16) obtained expressions for the moments of the chromatographic curve, c(L, t), as follows:

$$\mu_1 = (L/u)(1+\delta_o) + \frac{t_0}{2} \tag{3}$$

$$\mu_2' = (2L/u)\left[\frac{E_A}{\varepsilon_p}(1+\delta_0)^2\frac{1}{u^2} + \delta_1\right] + \frac{t_0^2}{12} \tag{4}$$

where

$$\delta_0 = \frac{\varepsilon_p}{m}\left(1 + \frac{\rho_p K_A}{\varepsilon_p}\right) \tag{5}$$

$$\delta_1 = \frac{\varepsilon_p}{m}\left[\frac{\varepsilon_p}{15}\left(1 + \frac{\rho_p K_A}{\varepsilon_p}\right)^2\left(\frac{1}{(D_e/R^2)} + \frac{5R}{k_f}\right) + \frac{\rho_p K_A^2}{\varepsilon_p k_{ads}}\right] \tag{6}$$

$$\mathrm{m} = \varepsilon_{\mathrm{b}}/(1 - \varepsilon_{\mathrm{b}}) \tag{7}$$

Here, t_0 is the retention time of a nonretained component (thiourea in this study).

Schneuder and Smith (1968) (17) proposed a method for estimating the equilibrium and kinetic parameters from the first absolute and second central moments based on the response signals from a series of measurements with varied flow rates.

First Moment Analysis

For an inert (nonretained) tracer, the first moment becomes as follows:

$$(\mu_1)_{inert} = (L/u)\left(1 + \frac{\varepsilon_p}{m}\right) \tag{8}$$

Subtracting Eq. (8) from Eq. (3) gives the following equation:

$$\Delta\mu_1 = \mu_1 - (\mu_1)_{inert} = \frac{\varepsilon_p}{m}\rho_p K_A\left(\frac{L}{u}\right) + \frac{t_0}{2} \tag{9}$$

According to Eq. (9), a plot of the reduced moment ($\Delta\mu_1 - t_0/2$) vs. L/u should be a straight line through the origin. Therefore, the adsorption equilibrium constant, K_A, can be obtained from the slope of the straight line.

In the interpretation and analysis of chromatographic data, it is assumed that system isotherm is linear. The assumption of linearity is a valid approximation provided that the concentration change over which the response is measured is sufficiently small (15, 16). Hence, for linear isotherm systems, first moment data can give reasonably accurate adsorption equilibrium constants.

Second Moment Analysis

Equations (4) to (7) can be used to obtain axial dispersion coefficient (E_A) and to evaluate the distribution of intraparticle diffusion coefficient (D_e), mass transfer coefficient (k_f), and intrinsic adsorption rate constant (k_{ads}).

According to Eq. (4), a plot of ($\mu_2' - t_0^2/12$) ($u/2L$) vs. ($1/u^2$) will be a straight line. Then, the axial dispersion coefficient, E_A, can be determined by the slope of this plot, $(E_A/\varepsilon_p)(1+\delta_0)^2$. The intercept of the line is related to the adsorption rate constant (k_{ads}), effective diffusivity (D_e), and mass transfer coefficient (k_f). However, the rate of physical adsorption is usually very fast, thus the contribution of the adsorption rate constant to the second moment can be neglected (14, 18, 19).

This second moment analysis is based on the assumption that both E_A and k_f are not influenced by velocity. This assumption can be satisfied at the condition of low Reynolds number and verified experimentally (17).

RESULTS AND DISCUSSION

To investigate the effect of temperature and eluent composition, many chromatographic responses were obtained from the experiments. Figure 1(a) shows the representative response peaks for the mixture of toluene and *p*-xylene at 308 K, 8 : 2 (methanol : water, v : v) eluent composition, and 4 mL/min flow rate. The moment analysis could be applied for a peak showing a Gaussian-type. The value of t_0 was obtained from the retention time of the response peak for thiourea, nonretained component, in Fig. 1(b).

Adsorption Equilibria

To obtain adsorption equilibrium constants from experimental chromatographic peaks, the first moment analysis was applied to the elution peak. Since the experiments have been performed in a linear range of adsorption isotherm, the result of first moment was presented under the linear shape as shown in Figs. 2 and 3. Therefore, the moments of the response peaks could be reasonably used to interpret the data.

Figure 2 shows the dependence of the reduced first absolute moment on L/u at several temperatures. Each point in the figure was determined by a chromatographic experiment at a certain temperature and flow rate and was performed at least three times to ensure reproducibility. For all the experiments, the eluent composition was fixed to 8 : 2 (methanol : water, v : v). At each temperature, the chromatographic curves were obtained at six different flow rates (2, 2.5, 3, 4, 5, and 6 mL/min). The K_A values of toluene and *p*-xylene at each temperature were able to be determined from the slope of the plots by a least-square regression.

Figure 3 shows the dependence of the reduced first absolute moment on L/u at several eluent compositions and 308 K. As shown in Fig. 3, all the plots at a certain eluent composition were also linear. Therefore, by a linear regression, the K_A values of toluene and *p*-xylene at each eluent composition (9 : 1, 8 : 2, 7 : 3, and 6 : 4, $v_{methanol} : v_{water}$) were determined.

The dependence of adsorption equilibrium on the temperature and the eluent composition is shown in Fig. 4.

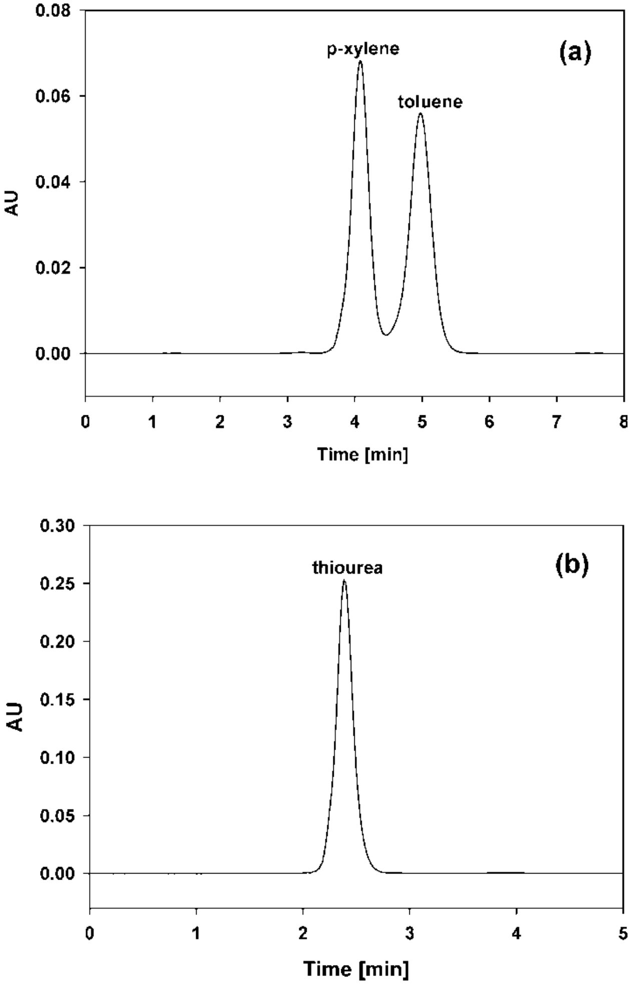

Figure 1. Chromatographic responses of (a) toluene/*p*-xylene mixture and (b) thiourea at 308 K and 8 : 2 (methanol : water, v : v) eluent composition (at 4 mL/min).

As shown in Fig. 4(a), the equilibrium constants of both components decreased with an increase in temperature. The equilibrium constants of *p*-xylene were much larger than those of toluene because *p*-xylene is a more adsorbable component than toluene on C_{18}-silica gel. However, since the significant reduction of the equilibrium constant with temperature was not observed in the experimental range, the difference of the equilibrium constant between both components was almost kept constant with the change of temperature. It implies that the temperature is not a crucial variable for the separation process in the toluene/*p*-xylene mixture.

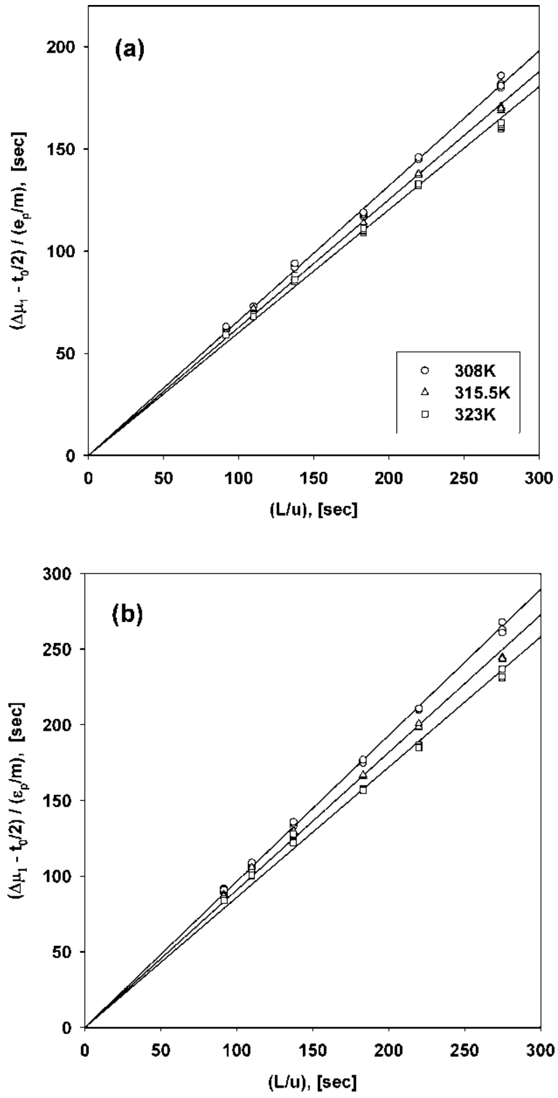

Figure 2. Dependence of the first moment of the chromatographic response curve on L/u at 308, 315.5, and 323 K: (a) toluene and (b) *p*-xylene (the eluent composition was fixed at 8 : 2, $v_{methanol} : v_{water}$).

Figure 4(b) shows the effect of eluent composition on the equilibrium constants of toluene and *p*-xylene at 308 K. As shown in the figure, the equilibrium constants decreased with increasing methanol ratio in the eluent. When the methanol ratio increased from 60 to 80%, the equilibrium constants of both components, especially *p*-xylene, steeply decreased. In addition, the

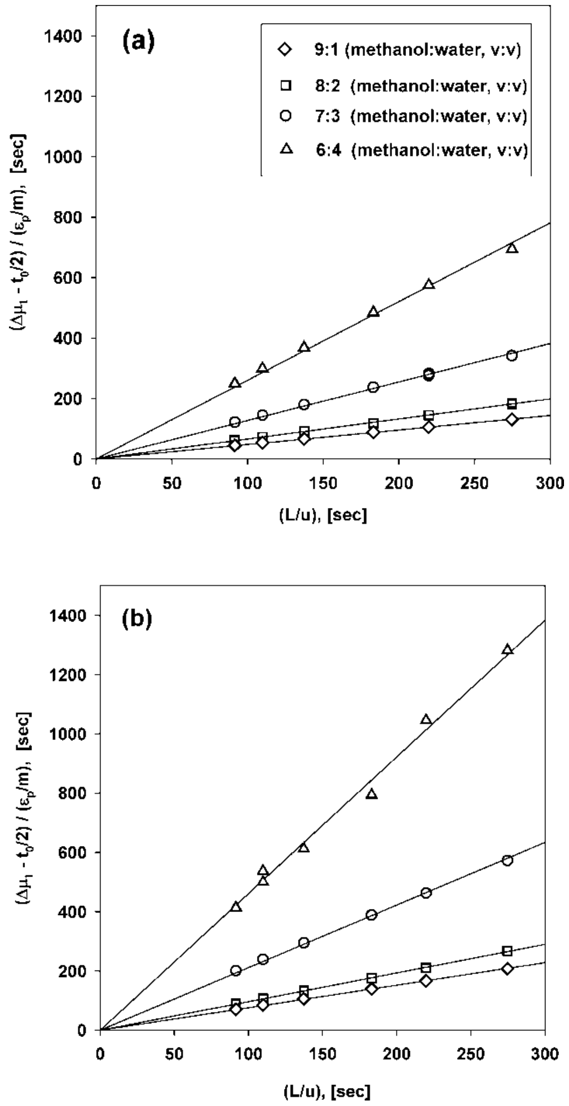

Figure 3. Dependence of first moment of chromatographic response curve on L/u at several eluent composition: (a) toluene and (b) *p*-xylene (temperature was fixed at 308 K).

difference of equilibrium constant between both components became small with an increase in the methanol ratio. However, when the methanol ratio increased from 80 to 90%, the equilibrium constants slightly decreased. Since the solid phase used, a reverse-phase C_{18}, was a non-polar material, the elution time decreased with a decrease of the solvent polarity.

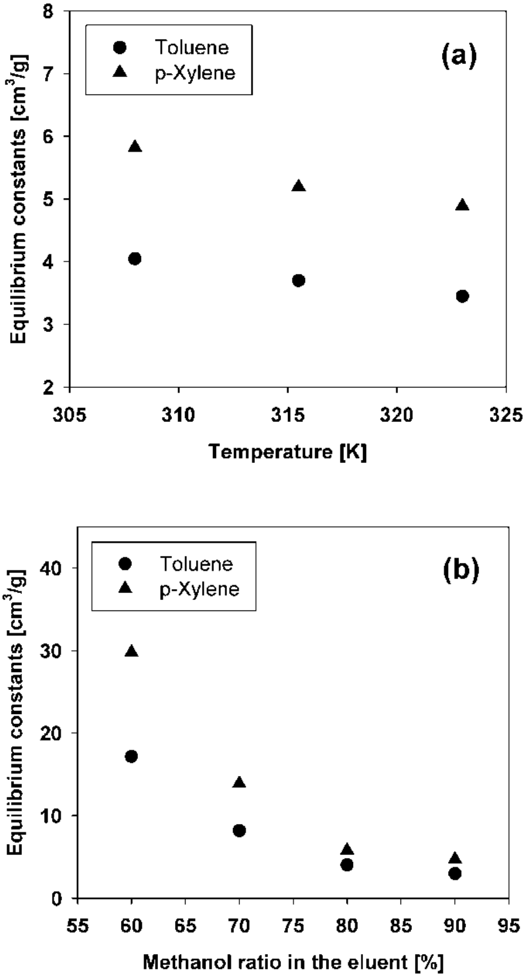

Figure 4. Effect of (a) temperature and (b) methanol ratio in the eluent (at 308 K) on the equilibrium constants of toluene and *p*-xylene.

Therefore, as the methanol ratio in the eluent was decreased, the internal profile of injected pulse proceeded slowly. As a result, it is expected that the eluent composition will act as a crucial variable in the adsorption equilibrium process.

Using the equilibrium constants calculated above, the adsorption isotherms of toluene and *p*-xylene on C_{18}-silica gel at 308, 315.5, and 323 K were obtained as shown in Fig. 5. From these linear isotherms, the adsorbed amounts of both components at a certain liquid concentration can be obtained. These results will be used for the prediction of the simulated moving bed process mentioned later.

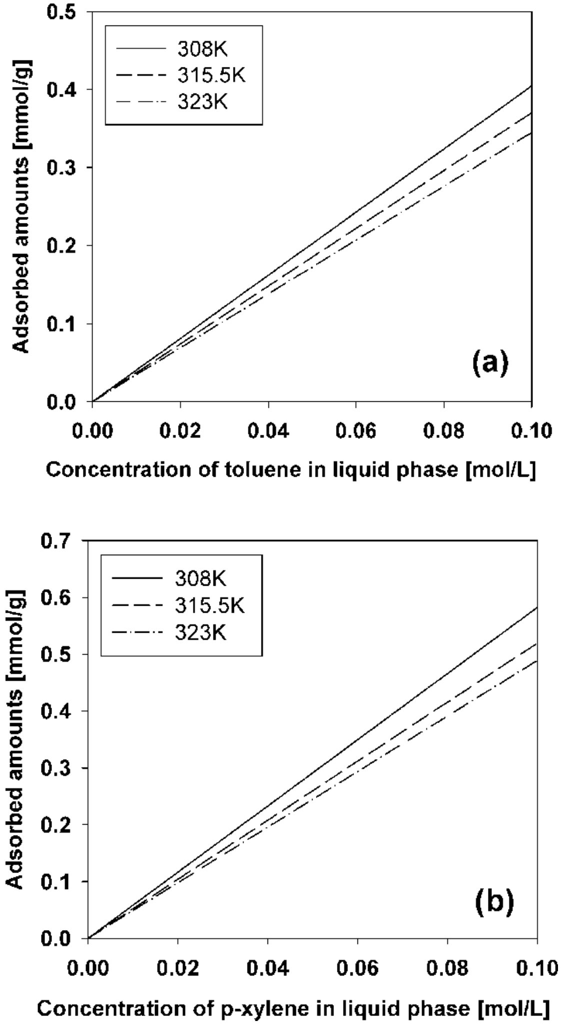

Figure 5. Equilibrium isotherms of (a) toluene and (b) *p*-xylene on C_{18}-silica gel at 308, 315.5, and 323 K.

According to the following Van't Hoff equation, the isosteric heat of adsorption (Q_{st}) of each component can be calculated from the temperature dependence of K_A in Fig. 5 (1).

$$K_A = K_{A0} \cdot \exp\left(\frac{-Q_{st}}{RT}\right) \tag{10}$$

Here, K_{A0} is K_A at $1/T = 0$ or $Q_{st} = 0$, R is the universal gas constant, and T is the absolute temperature.

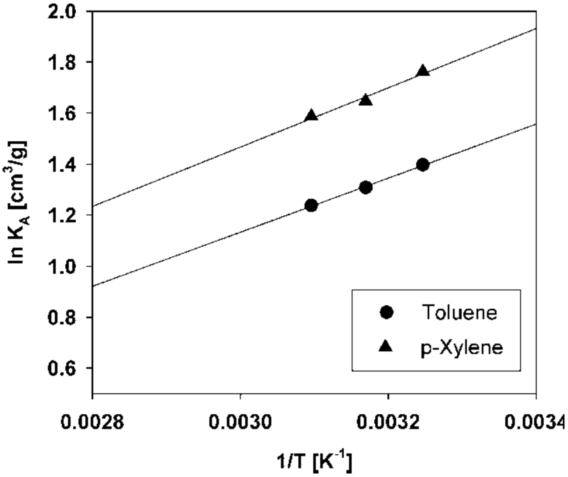

Figure 6. Van't Hoff's plot of adsorption equilibrium constant.

Figure 6 shows the Van't Hoff plot for the equilibrium constants using Eq. (10). The values of $-Q_{st}$, obtained from the slope of linear line, were ranged from 8.8 to 9.7 kJ/mol. These values are of the same order of magnitude as others previously reported for the same components in RP-HPLC systems using aqueous solutions of methanol (6.7 to 10.3 kJ/mol) (20). As shown in Table 4, the isosteric heat of adsorption of *p*-xylene was slightly larger than that of toluene and the values of K_{A0} derived from the intercept at $1/T = 0$ in Fig. 6 also showed the same trend.

An interesting variable that can be calculated from the equilibrium data are the capacity factor. The capacity factor of a solute is defined as the ratio of the moles of solute in the stationary phase to the moles of solute in the mobile phase. This factor can be represented as follows (21, 22):

$$k' = \frac{t^R - t_0}{t_0} \tag{11}$$

Here, t^R is the retention time of sample, and t_0 is the retention time of non-retained compound (dead time).

Table 4. Thermodynamic properties of retention equilibrium in RP-HPLC

Sample	$-Q_{st}$ (kJ/mol)	K_{A0} (cm^3/g)
Toluene	8.8	0.129
p-Xylene	9.7	0.133

Using these capacity factors of both components, the selectivity, α, can be calculated as follows:

$$\alpha = \frac{k'_{p\text{-}xylene}}{k'_{toluene}} \tag{12}$$

The results of the capacity factor and selectivity at each experimental condition were listed in Table 5. The capacity factors for both toluene and *p*-xylene slightly decreased with an increase of temperature while the selectivity did not show any correlation with temperature.

At 308 K, the capacity factors for both toluene and *p*-xylene showed the largest value at 6 : 4 methanol-water ratio, but the smallest value at 8 : 2 methanol-water ratio. However, the selectivity was a maximum at 7 : 3 methanol-water ratio, but a minimum at 8 : 2 methanol-water ratio, which was ranged from 1.48 to 1.68 according to the change of eluent composition at 308 K.

Adsorption Kinetics

The second moment analysis for transport properties was applied to the experimental chromatographic peak. To analyze the experimental data, Eq. (4) was changed into the following form (14, 23, 24):

$$\frac{\mu_2' - t_0^2/12}{2(L/u)} = \frac{E_A}{\varepsilon_p}(1+\delta_0)^2\frac{1}{u^2} + \delta_1 \tag{13}$$

Figure 7 shows the dependence of the second moment on $1/u^2$ at 308, 315.5, and 323 K for *p*-xylene as a representative result. For all the experiments, the eluent composition was fixed to 8 : 2 (methanol : water, v : v). As shown in Fig. 7, the second moment results were more scattered than the first moment results because higher moments are more sensitive to data analysis. However, they showed reasonably straight lines that were enough to evaluate the transport properties by the second moment. Therefore, the E_A values (axial dispersion coefficients) of toluene and *p*-xylene at each temperature (308, 315.5, and 323 K) were obtained from the slope of the plots by a linear regression.

The intercept of Eq. (13), δ_1, is related to a combination of the adsorption rate constant (k_{ads}), effective diffusivity (D_e), and mass transfer coefficient (k_f). As mentioned before, since the rate of physical adsorption is usually very fast, the contribution of the adsorption rate constant to the second moment was neglected (10, 14, 15). However, one of the mass transfer coefficient and the effective diffusivity has to be determined by another method in order to evaluate the other one from Eq. (13).

The mass transfer coefficient depends, in general, on the velocity. However, Schneider and Smith (1968) (17) used the Wakao-Kaguei

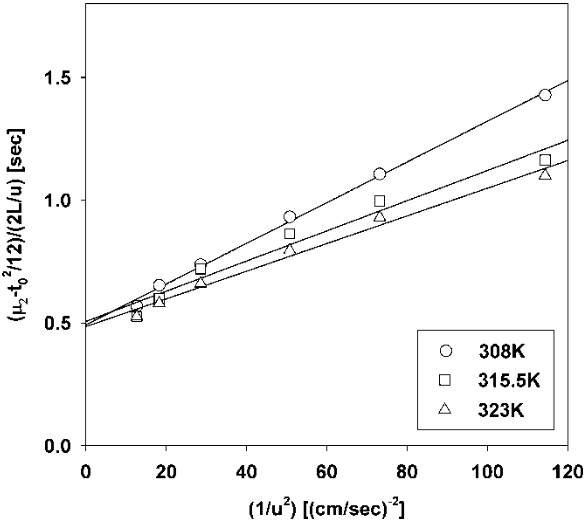

Figure 7. Dependence of the second moment of the chromatographic response curve on $1/u^2$ at several temperatures in the 8 : 2 (methanol : water, v : v) eluent composition for the case of *p*-xylene.

correlation for the analysis of their chromatographic data, as mass transfer coefficient is assumed to be independent on velocity at low Reynolds numbers. In this study, the Reynolds numbers were small enough to assume the independence of the mass transfer coefficient on velocity for all the experimental conditions. Therefore, the mass transfer coefficients could be calculated by the following Wakao-Kaguei correlation (19):

$$Sh = 2 + 1.1Sc^{1/3} \cdot \mathrm{Re}_p^{0.6} \tag{14}$$

Here, $Sh = (\mathrm{k_f\ d_p})/\mathrm{D_m}$, $Sc = \mu/(\rho\ \mathrm{D_m})$, and $\mathrm{Re}_p = (\rho\ \mathrm{d_p\ u})/\mu$.

To use the above correlation, mixture viscosity, mixture density, and molecular diffusivity were needed. The viscosity and density of solvent mixture were calculated by a mixing rule using the values of pure solvent shown in Table 3 (25). The molecular diffusivity of a solute in methanol-water mixture was estimated by the Scheidel equation (26):

$$\frac{D_m \mu_{mix}}{T} = \frac{K}{V^{1/3}} \tag{15}$$

$$K = (8.2 \times 10^{-8})\left[1 + \left(\frac{3V_{sol}}{V}\right)^{2/3}\right] \tag{16}$$

Here, V is the molar volume of solute at a standard boiling point. If V is less than 2.5 V_{sol} at organic solvent, K is 17.5×10^{-8}.

Once the mass transfer coefficients were calculated by the above method, the effective diffusivities could be evaluated by using Eq. (6). Table 6 shows the axial dispersion coefficients, the mass transfer coefficients, and the effective diffusivities obtained from the method stated above. In the case of 8 : 2 eluent composition, the axial dispersion coefficients of toluene and *p*-xylene showed the maximum value at 315 K. The axial dispersion coefficients of toluene decreased with increasing methanol ratio from 60 to 80%, and then slightly increased with increasing methanol ratio from 80 to 90%. Also, those of *p*-xylene slightly increased with increasing methanol ratio from 60 to 80%, and then steeply increased with increasing methanol ratio from 80 to 90%.

The mass transfer coefficients and effective diffusivities of both components showed a similar trend to the selectivity in Table 5, which was the lower value at the condition of lower selectivity. In addition, these values slightly decreased with an increase in temperature, but the effect of temperature on both transport properties was trivial. Even though the effective diffusivity and mass transfer coefficient showed minimum values at 8 : 2 methanol-water ratio, the differences in the resulted values were too small in the experimental range to consider the kinetic effects.

Separation of Toluene and *p*-Xylene by SMB Process

The equilibrium and kinetic results can be applied for the design and prediction of the SMB process. In this study, based on the above results, the operating condition for the toluene/*p*-xylene separation in the SMB process was determined by the triangle theory (11). As shown in Table 5, at 308 K, the capacity factors for both toluene and *p*-xylene showed the smallest values at 8 : 2 methanol-water ratio, but the selectivity was a minimum (1.48) at 8 : 2 methanol-water ratio. In an SMB process, the selectivity of

Table 5. Capacity factors and selectivities for toluene and *p*-xylene

T (K)	Methanol : Water (v : v)	Capacity factor, k'(-)		Selectivity
		Toluene	*p*-Xylene	
308.0	9 : 1	0.82	1.30	1.59
	8 : 2	0.64	0.95	1.48
	7 : 3	1.20	2.01	1.68
	6 : 4	2.49	4.04	1.62
315.5	8 : 2	0.61	0.86	1.41
323.0	8 : 2	0.58	0.84	1.45

Table 6. Transport properties

T (K)	Methanol : Water (v : v)	$E_A \times 10^{-4}$ (cm^2/sec)	$k_f \times 10^{-2}$ (cm/sec)	$D_e \times 10^{-5}$ (cm^2/sec)
Toluene				
308.0	9 : 1	3.124	2.746	2.239
	8 : 2	2.767	2.614	2.121
	7 : 3	2.938	2.727	2.397
	6 : 4	3.385	3.082	2.688
315.5	8 : 2	2.907	2.574	2.014
323.0	8 : 2	2.653	2.545	1.918
p-Xylene				
308.0	9 : 1	5.293	2.602	2.101
	8 : 2	3.296	2.466	1.979
	7 : 3	3.186	2.615	2.172
	6 : 4	3.165	2.761	2.364
315.5	8 : 2	4.831	2.370	1.826
323.0	8 : 2	3.149	2.287	1.687

1.48 is enough to separate both components. Furthermore, smaller capacity factor leads to lower eluent consumption due to shorter switching time. Hence, the eluent composition was chosen as 8 : 2 (methanol : water, v/v). On the other hand, the temperature dependence of the capacity factors was so small that the lowest temperature of 308.0 K was selected as the operating temperature of the SMB process. The determined switching time and flow rates were as follows: switching time for each column was $t^* = 2.52$ min, and flow rates of four pumps were Q_F (feed flow rate) = 1.00 mL/min, Q_D (desorbent flow rate) = 1.72 mL/min, Q_{II} (flow rate in zone II) = 6.20 mL/min, and Q_{IV} (flow rate in zone IV) = 5.67 mL/min. A small pilot-scale SMB, KNAUER CSEP® 9116 (KNAUER, Berlin, Germany), was used for the separation of toluene/*p*-xylene mixture. The equilibrium-dispersive model with a linear isotherm (27) was used for the prediction of the purity and the product concentration histories of the experimental results.

Figure 8 shows the transient purity histories of raffinate (toluene) and extract (*p*-xylene) under the above condition. As shown in this figure, the cyclic steady-state approached at 10 cycles and the product purities of both components were more than 99.9%. And the simulated results showed a good agreement with the experimental results.

Figure 9 shows the transient concentration histories of raffinate and extract. The symbols represent the experimental concentrations at each cycle. The thin lines show the original SMB zigzag concentration profiles predicted by simulation, while the thick lines represent the average

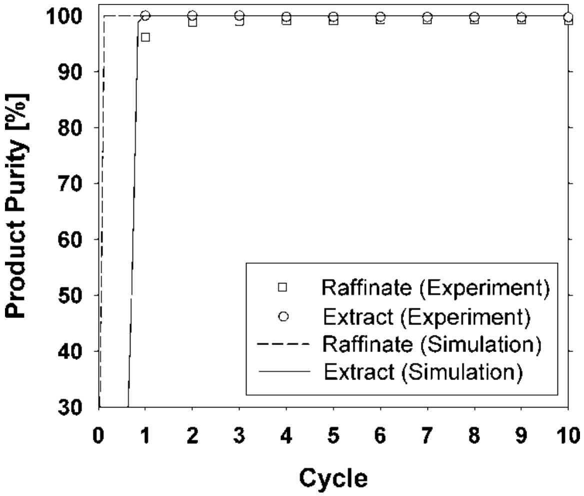

Figure 8. Product purities of raffinate (toluene) and extract (*p*-xylene) by simulated moving bed process (methanol : water = 8 : 2, $Q_F = 1.00$ mL/min, $Q_D = 1.72$ mL/min, $Q_{II} = 6.2$ mL/min, $Q_{IV} = 5.67$ mL/min, Switching time = 2.52 min/column).

concentration for each switching period. The experimental result for the raffinate was slightly larger than the simulated result. However, in the case of the extract, the simulated result was slightly smaller than the experimental result. These deviations may be caused by slight leanings of internal profiles toward raffinate port, which is resulted from the column-to-column variation. In addition, it was assumed in the simulation that all the eight columns of the SMB process had identical property. However, in the actual SMB experiment, the column properties, such as retention time and separation resolution, were somewhat different from each other.

In spite of these experimental factors, the simulated results reasonably predicted the experimental results of the SMB process. It implies the validation of the equilibrium and kinetic parameters obtained from the chromatographic method.

CONCLUSION

The adsorption equilibrium and transport properties of toluene and *p*-xylene in a packed chromatographic column were studied at various temperatures and eluent compositions.

From the first moment analysis, the adsorption equilibrium constants were obtained. The adsorption amount and affinity of *p*-xylene on the Eurosil 100-30-C_{18} were higher than those of toluene. Although the equilibrium constants of toluene and *p*-xylene decreased with an increase in temperature, the

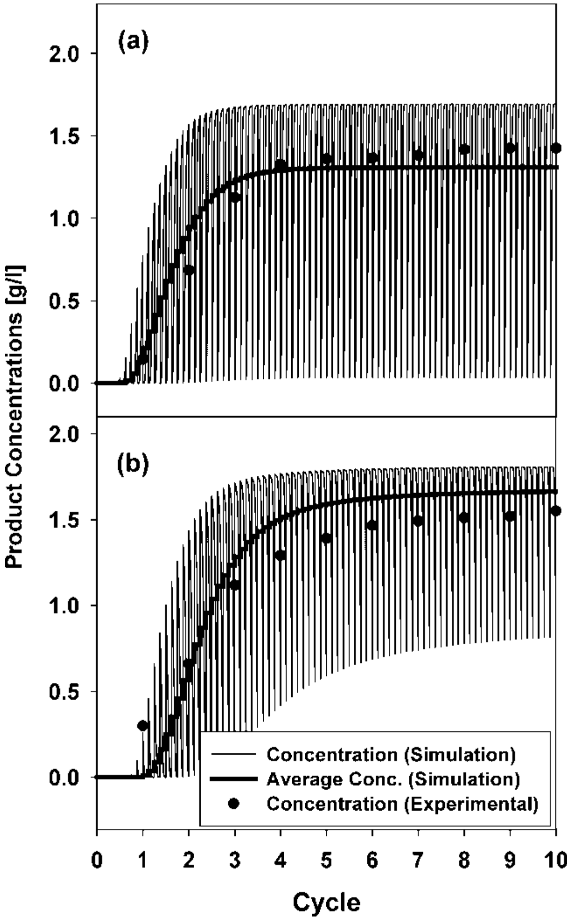

Figure 9. Product concentration profiles of (a) raffinate and (b) extract by simulated moving bed process (same condition with Fig. 8).

temperature was not a crucial variable in the adsorption equilibrium process because the trivial difference in the selectivity was only observed in the experimental range. On the other hand, the eluent composition acted as a crucial variable in the adsorption equilibrium process because the equilibrium constants of both components significantly decreased with an increase in methanol ratio of the eluent.

The transport properties were obtained from the second moment analysis. The effective diffusivity and mass transfer coefficient of both components slightly decreased with an increase in temperature. However, the differences in the effective diffusivities and mass transfer coefficients were so small in the experimental range that these differences could be negligible.

Based on the equilibrium and kinetic results, the operating condition for the toluene/*p*-xylene separation by the SMB process was determined. From the simulated and experimental results, it was confirmed that toluene and *p*-xylene could be successfully separated by the SMB process. Also, the simulated results, using equilibrium and kinetic parameters obtained from the moment method, predicted well the experimental SMB results.

NOMENCLATURE

c	adsorbable solute concentration in the liquid (mol/cm^3)
D_e	effective diffusivity (cm^2/sec)
D_m	binary molecular diffusivity (cm^2/sec)
d_p	particle diameter (cm)
E_A	axial dispersion coefficient (cm^2/sec)
K_A	adsorption equilibrium constant (cm^3/g)
k_{ads}	adsorption rate constant (cm^3/g sec)
k_f	mass transfer coefficient (cm^3/g sec)
k'	capacity factor (-)
L	bed length (cm)
m	$\varepsilon_b/(1-\varepsilon_b)$ (-)
Q_{st}	isosteric heat of adsorption (kJ/mol)
R	radius of pellet (cm); universal gas constant = 8.314 J/(mol K)
Re_p	Reynolds number = $\rho_{mix}\, d_p\, u/\mu_{mix}$ (-)
Sc	Schmidt number = $\mu_{mix}/\rho_{mix}\, D_m$ (-)
Sh	Sherwood number = $k_f\, d_p/D_m$ (-)
t	time (sec)
t^R	retention time (sec)
t_0	retention time of a nonadsorbable component (sec)
T	absolute temperature (K)
u	interstitial velocity (cm/sec)
V	molar volume of solute at standard boiling point (cm^3/mol)

Greek Symbols

α	selectivity (-)
ε_p	void fraction of particle (-)
ε_b	void fraction of bed (-)
μ_{mix}	viscosity of solvent mixture (g/cm sec)
μ_1	first absolute moment (sec)
$\mu_2{}'$	second central moment (sec^2)
ρ_p	particle density (g/cm^3)

ACKNOWLEDGMENT

The financial support of the Korea Research Foundation Grant (KRF-2003-005-D00001) is gratefully acknowledged.

REFERENCES

1. Miyabe, K., Sotoura, S., and Guiochon, G. (2001) Retention and mass transfer characteristics in reversed-phase liquid chromatography using a tetrahydrofuran-water solution as the mobile phase. *J. Chromatogr. A.*, 919: 231.
2. Jung, Y.A., Choi, D.Y., Hong, S.B., and Row, K.H. (2003) Mobile phase composition for resolving whey proteins in reversed-phase high performance liquid chromatography. *Korean J. Chem. Eng.*, 20: 705.
3. Kim, M., Way, J.D., and Baldwin, R.M. (2004) Effects of cross-linking and spacer groups on beta-cyclodextrin bonded liquid chromatographic separation. *Korean J. Chem. Eng.*, 21: 465.
4. Lee, K.N. (2003) Continuous separation of glucose and fructose at high concentration using two section simulated moving bed process. *Korean J. Chem. Eng.*, 20: 532.
5. Yoon, T.H. and Kim, I.H. (2004) Chiral separation of ketoprofen racemate by using Chirex® 3005 and Kromasil® CHI-II chiral column. *Korean J. Chem. Eng.*, 21: 521.
6. Zhang, Z., Mazzotti, M., and Morbidelli, M. (2004) Continuous chromatographic processes with a small number of columns: Comparison of simulated moving bed with Varicol, PowerFeed, and ModiCon. *Korean J. Chem. Eng.*, 21: 454.
7. Guiochon, G., Golshan-Shirazi, S., and Katti, A. (1994) *Fundamentals of Preparative and Nonlinear Chromatography*; Academic Press: Boston.
8. Minceva, M. and Rodrigues, A.E. (2003) Influence of the transfer line dead volume on the performance of an industrial scale simulated moving bed for p-xylene separation. *Separation Science and Technology*, 38: 1.
9. Ludemann-Hombourger, O., Bailly, M., and Nicoud, R.M. (2000) Design of a simulated moving bed: Optimal particle size of the stationary phase. *Separation Science and Technology*, 35: 285.
10. Storti, G., Masi, M., Carra, S., and Morbidelli, M. (1989) Optimal design of multicomponent countercurrent adsorption separation processes involving nonlinear equilibria. *Chem. Eng. Sci.*, 44: 1329.
11. Storti, G., Mazzotti, M., Morbidelli, M., and Carra, S. (1993) Robust design of binary countercurrent adsorption separation processes. *AIChE J.*, 39: 471.
12. Mazzotti, M., Storti, G., and Morbidelli, M. (1994) Robust design of countercurrent adsorption separation processes: 2. Multicomponent systems. *AIChE J.*, 40: 1825.
13. Mazzotti, M., Storti, G., and Morbidelli, M. (1996) Robust design of countercurrent adsorption separation: nonstoichiometric systems. *AIChE J.*, 42: 2784.
14. Lee, C.H. and Holder, G.D. (1995) Use of supercritical fluid chromatography for obtaining mass transfer coefficients in fluid-solid systems at supercritical conditions. *Ind. Eng. Chem. Res.*, 34: 906.
15. Kubin, M. (1965) Beitrag Zur Theorie Der Chromatographie II: Einfluss der diffusion ausserhalb und der adsorption innerhalb des sorbens-korns. *Collection Czechoslov. Chem. Commun.*, 30: 2900.

16. Kučera, E. (1965) Contribution to the theory of chromatography linear non-equilibrium elution chromatography. *J. Chromatogr. A.*, 19: 237.
17. Schneider, P. and Smith, J.M. (1968) Adsorption rate constants from chromatography. *AIChE J.*, 14: 762.
18. Hsu, L.-K.P. and Haynes, H.W., Jr. (1981) Effect diffusivity by the gas chromatography technique: Analysis and application to measurements of diffusion of various hydrocarbons in zeolite. NaY. *AIChE J.*, 27: 81.
19. Wakao, N. and Kaguei, S. (1982) *Heat and Mass Transfer in Packed Beds*; Gordon, Breach, Ed.; Sci. Publications: New York.
20. Miyabe, K. and Suzuki, M. (1995) Chromatographic study on liquid-phase adsorption on octadecylsilyl-silica gel. *AIChE J.*, 41: 548.
21. Lee, J.H., Choi, Y.S., and Row, K.H. (1990) The capacity factors and efficiency in preparative high performance liquid chromatography. *Chemical Industry and Technology*, 8: 425.
22. Row, K.H., Choi, D.K., Hwang, K.Y., and Lee, Y.Y. (1990) The separation by using the chromatographic method. *Chemical Industry and Technology*, 8: 425.
23. Wakao, N. and Funazkri, T. (1978) The effect of fluid dispersion coefficients on particle-to-fluid mass transfer coefficients in packed bed—Correlation of Sherwood numbers. *Chem. Eng. Sci.*, 33: 1375.
24. Miyabe, K. and Suzuki, M. (1992) Chromatography of liquid-phase adsorption on octodecylsilyl-silica gel. *AIChE J.*, 38: 901.
25. Reid, R.C., Prausnitz, J.M., and Poling, B.E. (1986) *The Properties of Gases and Liquids*; McGraw-Hill: New York.
26. Suzuki, M. (1990) *Adsorption Engineering*; Kodansha Ltd.: Tokyo.
27. Mihlbachler, K., Fricke, J., Yun, T., Seidel-Morgenstern, A., Schmidt-Traub, H., and Guiochon, G. (2001) Effect of the homogeneity of the column set on the performance of a simulated moving bed unit, I. Theory. *J. Chromatogr. A.*, 908: 49.